Drill Hole Optimization for Augmenting Strucutral Integrity

NeerajBisht*, SuvamGairola, ShivamShekhawat, Deep Darshan, NiteshAithani
*Department of Mechanical Engineering, GB Pant University of Agri. & Tech., Pantnagar, PIN - 263145, India

Abstract

Strucutres develop cracks during the course of there life resulting in catastrophic failures.This can be reduced by drilling holes near the crak tip. Here the aspect of optimal position and size of the drill hole has been analysed. Addtionally the effect of supplementary hole has also been made. Finite element code ANSYS was used for the analysis. To verify the fracture capabilities of ANSYS the results were corroborated using photoelastic techniques. It was observed that reduction in stress intensity factor to a great extent depends upon the position of the stop hole. Also it was observed that as the radius of the crack was increased the stress intensity factor increased. Creating supplementary hole further reduced the stress intewnsiy factor. So it can be concluded that for employing the concept of drill hole its position and size should be accurately determined.

Keywords: Stress intensity factor, photoelasticity, finite element method, drill hole, optimization

1. Introduction

Development of cracks in a structure during its service period has resulted in catastrophic failures. To prevent these failures these parts have to be replaced. This, however is impractical at times as the cost and time of replacement amy be too high. Various methods have been proposed to counter this [1], fillig of cracks [2-4], repair by welding [5-7]. Another successful technique fo impede the effect of crack is drilling holes near the crack tip. Holes can be drilled at the crack tip reducing singukarity or at some distance from the crack top thereby deflecting the crack propagation [8-10]. It has alsao been seen that stress intensity factor reduction becomes more pronounce under mode II loading [11]. Keeping in view the above findings an analysis of proper position and size of the crack has been analysed. Also to observe the effect of mixed mode loading supplementary hole has been drilled near the first drilled hole and its position has been varied. Aslo the effect of size of ther hole ahs been studied at the optoimized position of the first drill hole. The analysis has been made using ANSYS Parametric Design Language (APDL).To verify theaccuracy of APDL and to arrivce at the optimized meshing photoelastic technique has been used [12]. The photoelastic technoique has been used by amnyrersearchers to solve fracture mechanics problems[13-15].To obtain the stress intensity factor aprogram was written in FRREMAT and an over deterministic [14] approach was used to hae higher accuracy in the results.

2. Experimental Procedure

The techniques used for ythe analysis of the problem are described below.

2.1 Photoelastic Experiment

Photo elastic technique depens upon the ability of certain materials to become optically anisotropic when under load. The most important parameter worth considering while selecting the photoelastic material is the material fringe value. In this case epoxy resin (Araldite) has been used for the analysis. The method as discussed in reference [16-18] has beenused to prepare the material and specimens.

2.1.1 Material Fringe value

The material fringe values are determined using the diametral compression technique. For this a circular disc of 60 mm diameter was prepared amd examined under a circular polariscope. Figure 1 shows the fringes produced.

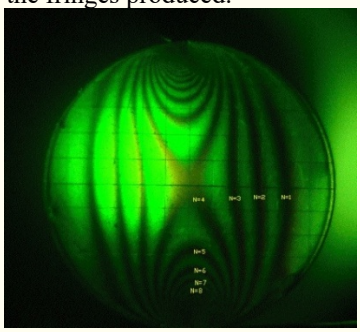

Fig. 1

The material fringe value was calculated as follows:

$$f_\sigma = \frac{8P}{\pi dN}$$

2.1.2 Specimen Geometry

The specimen of size 100 mm X 50 mm X 10 mm were prepared from epoxy. Slits of length 14 mm were cut using hag saw blade,futher pre-cracking upto 16 mm was done using razor blade. Loads of 200 N and 300 N were applid in uniaxial tensiuon as shown in Fig. 2.

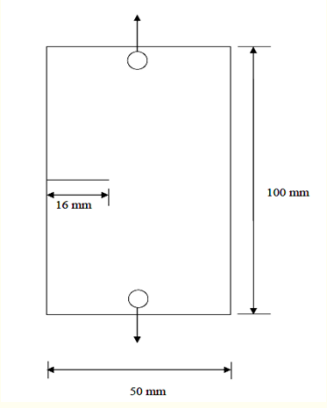

The fringes obtasined under 200N load are shown in Fig.3

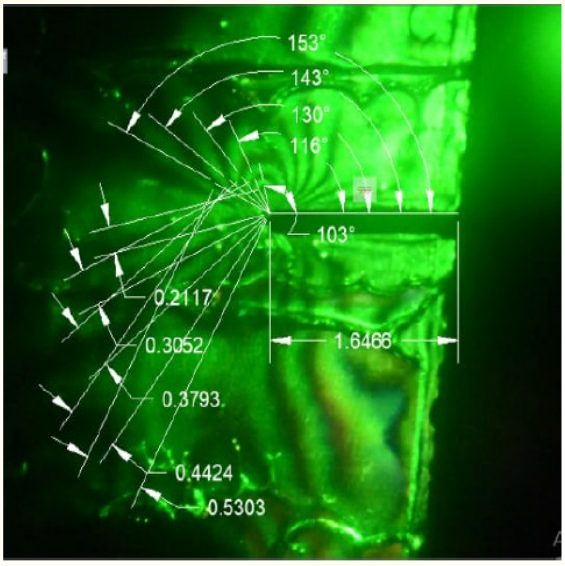

The pictures were imported into the CAD software and various points were considered and parameters related to them were evaluated.

2.1.3 Determination of stress field parameters

The stress optic law relates the fringe order N and principal stresses σ1 and σ2 as [14].

$$\frac{\sigma_1 - \sigma_2}{2} = \left(\frac{Nf_\sigma}{h}\right)^2 \qquad (3.1)$$

where h = specimen thickness, N = fringe order, f_σ= fringe value

For the purpose of study, the stresses in the local neighbourhood of a crack tip can be approximated by [14].

$$\sigma_{xx} = \frac{1}{\sqrt{2\pi r}}\left[K_I \cos\frac{\theta}{2}\left(1 - \sin\frac{\theta}{2}\sin\frac{3\theta}{2}\right) - K_{II}\sin\frac{\theta}{2}\left(2 + \cos\frac{\theta}{2}\cos\frac{3\theta}{2}\right)\right] \quad (3.2)$$

$$\sigma_{yy} = \frac{1}{\sqrt{2\pi r}}\left[K_I \cos\frac{\theta}{2}\left(1 + \sin\frac{\theta}{2}\sin\frac{3\theta}{2}\right) + K_{II}\sin\frac{\theta}{2}\cos\frac{\theta}{2}\cos\frac{3\theta}{2}\right] \quad (3.3)$$

$$\tau_{xy} = \frac{1}{\sqrt{2\pi r}}\left[K_I \sin\frac{\theta}{2}\cos\frac{\theta}{2}\cos\frac{3\theta}{2} + K_{II}\sin\cos\frac{\theta}{2}\left(1 - \sin\frac{\theta}{2}\sin\frac{3\theta}{2}\right)\right] \quad (3.4)$$

where r and θ are the polar coordinates with the origin defined at the crack tip.The maximum in-plane shear stress τ_m is related to the Cartesian components of stress as:

$$(2\tau_m)^2 = (\sigma_{yy} - \sigma_{xx})^2 + (2\tau_{xy})^2 \qquad (3.5)$$

Substituting eq (3.2-3.4) into eq (3.1) gives the relationship which defines the isochromatic fringe pattern in the local field near the crack tip as:

$$\left(\frac{Nf_\sigma}{h}\right)^2 = \frac{K_I^{\,2}}{8\pi r}sin^2\theta + \frac{K_{II}^{\,2}}{8\pi r}(4 - 3sin^2\theta) + \frac{K_I K_{II}}{2\pi r}\sin\theta cos\theta \qquad (3.6)$$

Eq.3.6 yields the relationship between fringe order N and stress intensity factor KI and KII.

2.1.4 Solution of the N-K relationship

In the present thesis work over deterministic approach has been employed [14]. In this approach data are selected from multiple arbitrary points (r1, θ1), (r2, θ2), (r3, θ3) …….. (rm, θm). The fitting process involves both Newton-Raphson method and the minimization process associated with the least square method is applied to solve the set of equations in terms of the corrections ΔKI and ΔKII. The method is presented below:-
Equation (3.6) can be rewritten as

$$f = \frac{K_I^{\,2}}{8\pi r} sin^2\theta + \frac{K_{II}^{\,2}}{8\pi r}(4 - 3sin^2\theta) + \frac{K_I K_{II}}{2\pi r}\sin\theta cos\theta - \left(\frac{Nf_\sigma}{h}\right)^2 \qquad (3.7)$$

Consider any arbitrary function hk of the form

$$h_k(K_I, K_{II}) = 0$$

$$[a] = -\begin{bmatrix} \frac{\partial f_I}{\partial K_I} & \frac{\partial f_I}{\partial K_{II}} \\ - & - \\ - & - \\ - & - \\ \frac{\partial f_I}{\partial K_I} & \frac{\partial f_I}{\partial K_{II}} \end{bmatrix} \qquad (3.13)$$

$$[\Delta K] = \begin{bmatrix} \Delta K_I \\ \Delta K_{II} \end{bmatrix} \qquad (3.14)$$

The least square minimization process is accomplished by multiplying from the left both sides of eqn (3.11) by the transpose of matrix$[a]$, to give

$$[a]^T[f] = [a]^T[a][\Delta K] \qquad (3.15)$$

$$\text{where} [d] = [a]^T[f] \qquad (3.17)$$

$$[c] = [a]^T[a] \qquad (3.18)$$

Finally the correction terms are given by:

$$[\Delta K] = [c]^{-1}[d] \qquad (3.19)$$

The solution of equation gives $\Delta K_I, \Delta K_{II}$ which are used to correct the initial estimates of KI, KII and obtain a better fit of the function f to m data points. Computer programs have been written in MATLAB to determine$\Delta K_I, \Delta K_{II}$.

2.1.5 Finite Element Modeling

APDL code was used in the present investigation. First the photoelastic experiments results were used to evaluate and corroborate ANSYS results. Then the geometry shown below was analysed to study the effect of different positions of the stop hole.
Plane strain conditons were assumed in the analysis.
The model was discretized using 8 node 2D element (iso parametric) having 2 degrees of freedom. To account for the stress singularity at the crack tip special discretization was used. The parameters involved in the meshing around the crack tip were varied to obtain an optimized meshing plan.

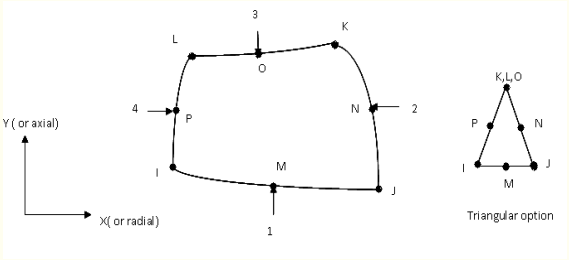

The stress intensity factors at a crack for a linear elastic fracture mechanics analysis is computed as follows:

$$K_I = \sqrt{2\pi}\frac{G}{k}\frac{|\Delta v|}{\sqrt{r}} \qquad (3.28)$$

$$K_{II} = \sqrt{2\pi}\frac{G}{1+k}\frac{|\Delta u|}{\sqrt{r}} \qquad (3.29)$$

$$K_{III} = \sqrt{2\pi}G\frac{|\Delta w|}{\sqrt{r}} \qquad (3.30)$$

Where, $\frac{|\Delta v|}{\sqrt{r}} \& \frac{|\Delta u|}{\sqrt{r}}$ were evaluated based on the nodal displacements and locations.

3. RESULTS AND DISCUSSION

Following results were obtained in the various tests conducted.

3.1. Experimental corroboration of ANSYS Results

Both photoelastic and ANSYS were employed to evaluate SIF for the geometry shown in Fig.2. From Fig.it can be seen that there is a very good agreement between results obtained from both the techniques. An error of 4% was observed between the photoelasticity and ANSYS results.

The values of N, r, θ were kept in the program and the result were obtained by runningthe program. The program converged in 15 steps using Gauss Siedel approach to solve the matrix and the error was minimized to 0.1%.

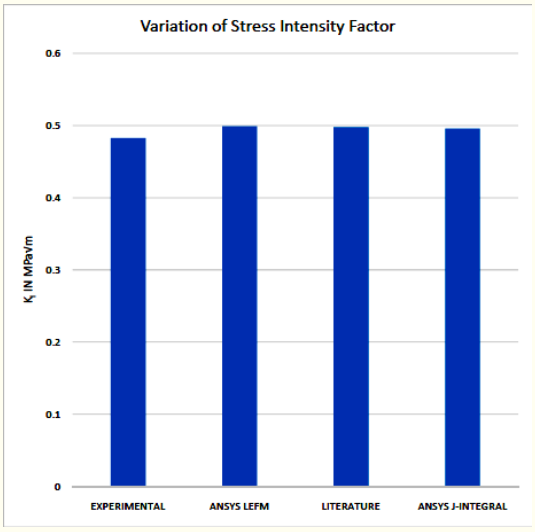

The obtained result was also verified using the J-integral approach. It was further verified using the analytical formula for a palte with a side crack under tension [32]. It can be observed that all the results are very close and the error involved is minimum.

3.2 Variation of Lateral Distance

In the first part the distance of the stop hole from the crack tip in the lateral direction was varied and the variation of SIF was studied. The Fig. shows this variation. The values of SIF have been normalized with a plate with a side crack in tension without hole.
It can be observed that when the distance of the stop hole is increased or as the crack tip and stop hole centre move further apart SIF starts decreasing. But the trend starts changing as the distance becomes so significant that presence of a hole is nullified. It can be seen that at a distance of 1mm from the crack tip the SIF has increased but its movement away from the crack tip results in decrease of SIF. Stop hole very close to the crack tip increases the stress around crack tip which is already high due to the stress singularity

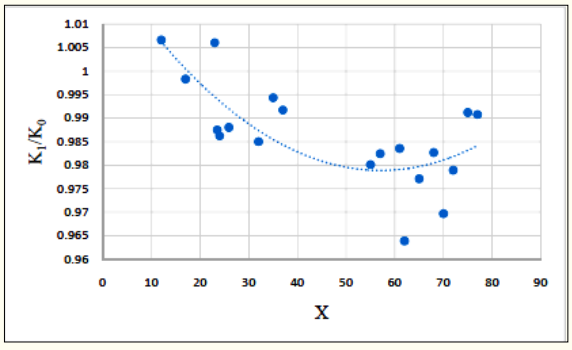

Since due to drilling of the hole effective cross sectional area decreases at the crack tip SIF increases. It was seen that for the present geometry considered the hole at a distance of 62 mm beyond which the effect of presemnce of hole becomes insignificant. Now keeping this lateral distance as constant perpendicular distance is varied and its optimum position is identified.

3.3 Variation of Perpendicular Distance

Now keeping x as constant the perpendicular distance is varied. FIG. shows this variation. It is observed that similar to the lateral distance variation the increase in diatance in the perpendicular direction also results in decrease of SIF.

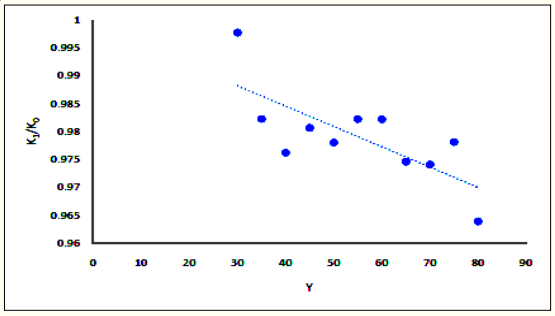

Presence of stop hole very near results in decrease of SIF however it decreases with further movement of the stop hole. However after a certain position its effect becomes insignificant and the SIF starts increasing ultimately reaching the previous value of SIF (plate without hole).

3.4 Variation of Radius

At this optimum position of the stop hole its radius was varied. The initial hole size considered was 0.5 mm (smaller size were not considered keeping in mind the practicaltiy). From Fig. it can be seen that as the hole size is increased from 0.5 mm the SIF drops but this drop is maintsained for a small range of 0.5 mm to 1mm. Further increase in the hole size results in increase of SIF. However it is still below the case of a palte without hole. This can be attributed to the fact that as radius increases effective cross section area decreases thereby increasing the net effective stress distribution around the crack tip.

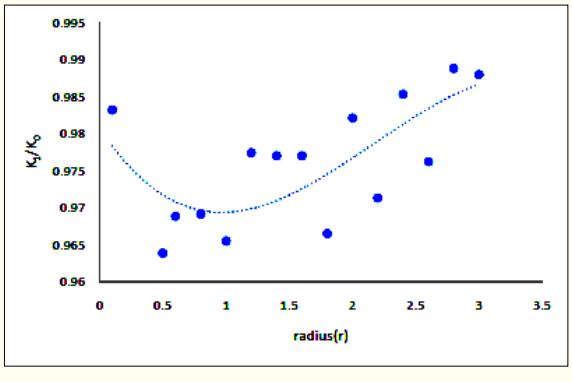

3.5 Effect of II nd stop hole

The effect of application of IInd stop hole was studied keeping the first stop hole at the optimum position. Fig. shows the results obtained. It can be seen form the Fig. that at first for a significant range there is no effect of second stop hole but as the two holes move cloaser to each other the SIF starts decreasing, this can be attributed to mixed mode loading occurring at the crack tip and this mode mixity results in impediment of crack

intensity. Comparing the two figs. It can also be seen that normalized value of SIF dropped from 0.97 to 0.96 with introduction of another hole.

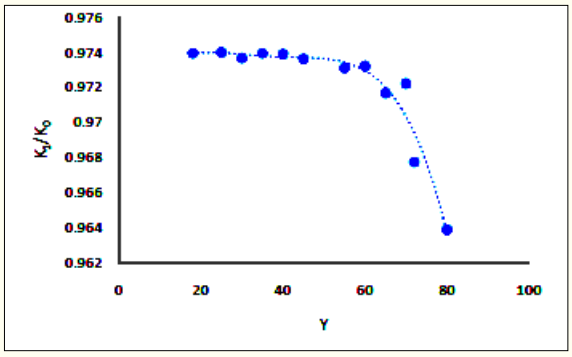

CONCLUSIONS

From the above discussions following conclusions can be made:

1. It is observed that variation of lateral and perpendicular position of stop hole has a profound impact on SIF, which would depend upon the specimen geometry and loading conditions.
2. Radius of drill hole is also significant, making the hole too large deteriorated the problem therefore estimation of hole size becomes impoartant.
3. Presence of a second stop hole is beneficial and helps in decreadsing the stress intensity factor.

Keeping in mind the above points it can be said that stop holetechnoique is abeneficial technique for life enhnancement. But the accurate estimation of its position and its size plays a pivotal role in degree of its effectiveness.

ACKNOWLEDGMENTS

This research did not receive any specific grant from funding agencies in the public, commercial, or not-for-profit sectors.

References

[1] Domazet Z. Comparison of fatigue crack retardation methods. Eng Fail Anal 1996;3(2):137–47.
[2] Elber W. Fatigue crack closure under cyclic tension. Eng. FractMech 1970;2:37–45.
[3] Sharp PK, Clayton JQ, Clark G. Retardation and repair of fatigue cracks by adhesive infiltration. Fatigue FractEng Mater Struct 1997;20(4):605–14.
[4] Shin CS, Cai CQ. A model for evaluating the effect of fatigue crack repair by the infiltration method. Fatigue FractEng Mater Struct 2000;23:835–45.
[5] Ayatollahi MR, Hashemi R. Mixed mode fracture in an inclined center crack repaired by composite patching. Compos Struct 2007;81:264–73.
[6] Mendez PF, Eagar TW. Penetration and defect formation in high-current arc welding. Weld J 2003;82(10):296–306.
[7] Liu C, Northwood DO, Bhole SD. Tensile fracture behavior in CO2 laser beam welds of 7075-T6 aluminum alloy. Mater Des 2004;25:573–7.
[8] Song PS, Shieh YL. Stop drilling procedure for fatigue life improvement. Int J Fatigue 2004;26:1333–9.
[9] Ghfiri R, Shi H, Guo R, Mesmacque G. Effects of expanded and non-expanded hole on the delay of arresting crack propagation for aluminum alloys.
Mater SciEng 2000;A286:244–9.
[10] Ghfiri R, Amrouche A, Imad A, Mesmacque G. Fatigue life estimation after crack repair in 6005 AT-6 aluminum alloy using the cold expansion hole technique. Fatigue FractEng Mater Struct 2000;23:911–6.
[11] Ayatollahi et al., Mixed mode fatigue crack initiation and growth in a CTspecimen repaired by stop hole technique. Engg.Fract. Mech. 145, 2015, 115-127.
[12] James W Dally
[13] Gope et al., Influence of crack offset distance on interaction of multiple collinearand offset edge cracks in a rectangular plate. The.& Appl. Fract. Mech., 2014, 19-29.
[14] R.J. Sanford, J.W. Dally, A general method for determining mixed mode stressintensity factors, Eng. Fract. Mech. 4 (1972) 357–366.
[15] K. Ramesh, S. Gupta, A.A. Kelkar, Evaluation of stress field parameters infracture mechanics by photoelasticity-revisited, Eng. Fract. Mech. 56 (1997) 25–45.
[16] V.K. Singh, P.C. Gope, Photoelastic determination of mixed mode stressintensity factor, J. Solid Mech. 3 (2009) 233–244.
[17] P.C. Gope, A. Thakur, Experimental investigation of crack growth directions in multiple crack problems, Fatigue Fract. Eng. Mater.Struct. 34 (2011) 804–815.
[18] V.K. Singh, P.C. Gope, Experimental evaluation of mixed mode stress intensity factor for prediction of crack growth by phoelastic method, J Failure Anal. Prevent. 13 (2013) 217–226.

Nomenclature

SIF stress intensity factor
APDL Ansys Parametric Design Language